Late Events in the Photocycle of Bacteriorhodopsin Mutant L93A

R. Tóth-Boconádi,* L. Keszthelyi,* and W. Stoeckenius†

*Institute of Biophysics, Biological Research Centre of the Hungarian Academy of Sciences, H-6701 Szeged, Hungary; and †Department of Biochemistry and Cardiovascular Research Institute, University of California, San Francisco, California, and Department of Chemistry, University of California at Santa Cruz, Santa Cruz, California USA

ABSTRACT In the photocycle of bacteriorhodopsin (bR) from *Halobacterium salinarum* mutant L93A, the O-intermediate accumulates and the cycling time is increased ~200 times. Nevertheless, under continuous illumination, the protein pumps protons at near wild-type rates. We excited the mutant L93A in purple membrane with single or triple laser flashes and quasicontinuous illumination, (i.e., light for a few seconds) and recorded proton release and uptake, electric signals, and absorbance changes. We found long-living, correlated, kinetic components in all three measurements, which—with exception of the absorbance changes—had not been seen in earlier investigations. At room temperature, the O-intermediate decays to bR in two transitions with rate constants of 350 and 1800 ms. Proton uptake from the cytoplasmic surface continues with similar kinetics until the bR state is reestablished. An analysis of the data from quasicontinuous illumination and multiple flash excitation led to the conclusion that acceleration of the photocycle in continuous light is due to excitation of the N-component in the fast N↔O equilibrium, which is established at the beginning of the severe cycle slowdown. This conclusion was confirmed by an action spectrum.

INTRODUCTION

The light-driven proton pump, bacteriorhodopsin (bR), occurs as crystalline patches (purple membrane (pm) in the cell membrane of *Halobacterium salinarum*. Bacteriorhodopsin undergoes a cyclic photoreaction with a transient all-*trans* to 13-*cis* isomerization of the retinal chromophore. This ''photocycle'' transports one proton from the cytoplasm to the medium, generating an outside-positive membrane potential. In addition to the ''ground state'' bR, six main intermediate states, labeled J, K, L, M, N, and O, characterized by their absorption spectra[1], have been identified in this photocycle. Substates of the intermediates, which are spectroscopically difficult to distinguish, and rapid thermal equilibria between them have been detected and/or postulated (see Chizhov et al., 1992, 1996). With better time and spectral resolution and the use of other techniques, we can expect to identify more substates of the main intermediates, and use them to further explore the molecular mechanism of this light-energy transduction. Electron and x-ray scattering, Resonance Raman and Fourier transform infrared spectroscopy, measurements of intramembrane currents, and mutation of single amino acids have so far proved to be most informative (for recent reviews, see Ebrey, 1993; Lanyi, 1993, 1997; Stoeckenius, 1999; Subramaniam et al., 1999; Luecke, 2000).

In the photocycle of bR mutant L93A, high concentrations of an O-like intermediate accumulate. This effect has been attributed to an inhibited reisomerization of its 13-*cis* retinal chromophore to the all-*trans* form, which causes an ~200-fold increase of the O-decay time. Nevertheless, in constant light, the L93A mutant pumps protons at rates comparable to wild-type bR (WTbR). This unexpectedly high pumping rate has been shown to be due to absorption of a second photon by an intermediate, presumably O, which reisomerizes the retinal and rapidly returns the molecule to the bR state completing the cycle (Subramaniam et al., 1991, 1997, 1999; Delaney et al., 1995; Delaney and Subramaniam, 1996).

In the course of work on the photoreactions of late photocycle intermediates, we reinvestigated the photocycle of L93A, and in addition to absorbance changes, measured the electric responses for excitations with flash and quasicontinuous illumination, and also the timing of proton release and uptake. We constrain analysis of our data by assuming that the photoreaction of L93A follows essentially the same reaction path as in WTbR, for which a good model exists, and that only the kinetics are affected by the mutation (see Discussion).

We found that the proton transport is completed only in the last step of the cycle and that the ''shortcut'' caused by the second photon originates at the N-intermediate. We also show data suggesting the presence of two consecutive O-intermediates. (*Note 2:* We use ''shortcut'' or ''bypass'' to characterize a reaction that effectively accelerates one or more transitions, completing the proton transport and restoring bR, as opposed to ''short circuit'' resulting from

Submitted August 1, 2001, and accepted for publication March 6, 2003.

Address reprint requests to Dr. Lajos Keszthelyi, Institute of Biophysics, Biological Research Centre of the Hungarian Academy of Sciences, H-6701 Szeged, Temesvari krt. 62, Hungary. Tel.: 36-62-599-615; Fax: 36-62-433-133; E-mail: kl@nucleus.szbk.u-szeged.hu.

[1]The photocycle intermediates were originally defined by their absorption maxima in the uv-visible range. When closer scrutiny and/or other techniques revealed substates, with the same or only slightly shifted maxima, they were usually distinguished by superscripts, subscripts, or numbering. Lately, conformational changes that preceded the absorbance changes have been detected in some intermediates, and these substates then have been labeled with the letter of the following state, which has led to confusion. To avoid this, we are still using the absorption maxima to identify an intermediate, which we feel is the obvious choice when dealing with photoreactions.

0006-3495/03/06/3848/09 $2.00

illumination of the earlier intermediates, which also restores the bR state fast but aborts the charge transport.)

MATERIALS AND METHODS

Pm was prepared by standard techniques from a L93A strain originally obtained from Dr. Subramaniam and maintained in Dr. Bogomolni's laboratory. Isolated pm fragments were oriented and immobilized in polyacrylamide gels as described by Dér et al. (1985). Gel slabs measuring $1.6 \times 1.6 \times 0.18$ cm^3 were cut and soaked in 100-cm^3 50 μM $CaCl_2$ solution at pH 7.5 at least overnight, and then placed in the same solution into the measuring cuvettes.

To excite the photocycle, we used a frequency-doubled Nd-YAG laser (Surelite I-10, Continuum, Santa Clara, CA) or an excimer laser-driven dye laser with dyes LC5000 coumarin 307 (500 nm), LC5400 coumarin 153 (540 nm), LC5900 rhodamin 6G (580 nm), LC6100 rhodamin B (605 nm), LC6600 sulforhodamin 101 (650 nm) (Lambda Physik EMG 101 MSC, Göttingen, Germany) and a 200-W tungsten lamp with heat and optical high pass filter (>560 nm) for quasicontinuous illumination or interference filters, to select monitoring beams. In some experiments, a xenon arc lamp (model A1010, Photon Technology International, Tornesch, Germany) with band-pass filter (transmission maximum at 536 nm, half transmissions at 490 and 605 nm) and also the 514 nm line of an argon ion laser (Stabilite 2016, Spectra-Physics, Mountain View, CA) were used. The light intensity was varied by neutral filters and measured with light meters (Alphametric dc1010, Karl Lambrecht, Chicago, or LI-250, LI-COR, Lincoln, NE). A homemade time generator controlled a mechanical shutter (opening and closing time ≈7 ms) for quasicontinuous illumination experiments.

Platinized Pt electrodes immersed into the solution picked up the electric signals in the ms time range, which, after appropriate filtering, were amplified by a homemade current amplifier based on a Burr-Brown 3554 operational amplifier, and digitized by a Thurlby DSA-524 computer-controlled transient recorder with 1024 channels (Thurlby Electronics., Huntington, UK) or a LeCroy 9310 L with 10,000 channels (LeCroy, Geneva, Switzerland).

Absorbances for the N-intermediate at 550 nm and O at 632 nm (with a He-Ne laser D5-LHP-151, Melles Griot, Arnhem, The Netherlands) were measured with a photomultiplier behind the sample and digitized as above. Because of the long lifetime of this mutant, we used monitoring beams of low intensity to minimize influence on the time courses (see Appendix Eq. 3). Repetition rates for averaging always were lower than 0.1Hz.

RESULTS

Single flash illumination

The early steps in the photocycle of L93A show small changes in kinetics of intermediates compared to WTbR, but these seem not to affect the reaction path, at least not in the later transitions (this was already seen by Delaney et al. (1995) but not commented). We shall in detail consider here only the later reactions in the millisecond–second range. Fig. 1 *A* shows the electric current response to laser flash excitation of the bR state. The early large negative and positive current components are similar to the electric signals measured for WTbR (Keszthelyi and Ormos, 1989). From 1 ms on, we could satisfactorily fit the curve with three exponentials, but that required two slow positive components with lifetimes of 260 and 1800 ms. (*Note 3:* Positive current is defined as transport of positive charge in the direction of pumping, i.e., from the cytoplasmic to the external side of the membrane.) The decay of O-absorbance (*dotted line* in Fig. 1 *B*) contains similar components (see Table1). (''O'' or ''O-intermediate'' in the context of this paper usually means a fast N↔O equilibrium, which is shifted toward O.) The difference in the lifetimes of electric

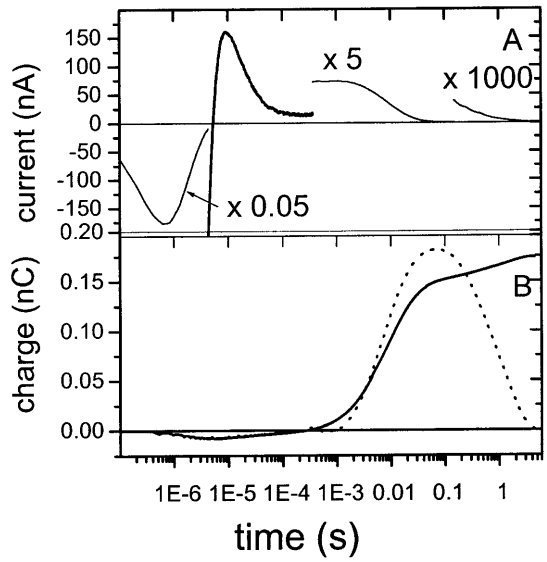

FIGURE 1 (*A*) Electric response to excitation of pm from mutant L93A oriented and immobilized in gels. (*B*) Solid line: time integral of the electric signal in *A* representing charge transport. Dotted line: absorbance of the O intermediate at 632 nm (data scaled). Lifetime values are given in Table 1. Exciting light: 530 nm flash of the Nd-YAG laser. Solution 50 μM $CaCl_2$, pH 7.5, 22°C. The same conditions apply to all figures, or differences are noted.

TABLE 1 Lifetimes of kinetic signal components for illuminated purple membrane from mutant L93A

Signal	τ_0	τ_1	τ_2	τ_3
Current, flash		(+) 6.3 ± 0.1	(+) 260 ± 10	(+) 1800 ± 100
Current, light off		n. d.	(+) 346 ± 10	(+) 1670 ± 410
A550		(r) 5.4 ± 0.1	(d) 383 ± 190	(d) 1500 ± 400
A632		(r) 10 ± 2	(d) 360 ± 10	(d) 1800 ± 100
D[H$^+$] L93A	(+) 0.75 ± 0.02	(−) 5.5 ± 0.1		(d) 1710 ± 30
D[H$^+$] WTbR	(+) 0.55 ± 0.01	(−) 3.40 ± 0.01		

Times are in ms. For electric signals, (+) indicates movement of positive charge in the pumping direction. Flash refers to laser flash excitation, light off at end of quasicontinuous illumination. A550 and A632 show O-absorbance measured at 550 and 632 nm. (r) and (d) indicate rise and decay. D[H$^+$] are proton concentration changes in the medium with (+) and (−) indicating release and uptake for mutant L93A and wild-type bR.

and optical data can be attributed to limited accuracy of the small, slow current measurements. The time integral of the current shows that most of the total charge transport occurs during the decay of M to N↔O, but the later slow components still account for 18% of the total charge transport (*solid line* in Fig. 1 *B*).

The charge motions with long lifetimes suggest that proton uptake also may continue through the O to bR transition, which is born out by experiment (Fig. 2 and Table 1). The lifetimes for the fast components of proton release and uptake agree well with the <1 ms and 6 ms components that Delaney et al. (1995) reported, but these authors cut their record at 40 ms. They attributed the slow continuing rise of the pH, recognizable in their Fig. 1, to baseline drift and concluded that proton translocation is completed in the transition to N. We find that at this point only ~40% of released protons have been taken up again and a slower uptake continues in parallel with the slow absorbance changes and current decay (Fig. 2). Similar biphasic proton uptake data were earlier found for other mutants with a disturbed D96 environment (Dioumaev et al., 2001).

Quasicontinuous illumination

Since the key observation prompting the closer investigation of L93A was the apparently unimpaired pumping in continuous light, we also recorded currents and O-absorbance changes under several seconds-long illuminations. In this quasicontinuous light, the current increases throughout the range of applied light intensities (Fig. 3 *A*). It reaches a maximum within the 7 ms opening time of the shutter, overshoots, and then falls back to a ''plateau'' value. Within the 7 ms shutter closing time, it rapidly drops to a low level. The small remaining current represents ~1% of the plateau value and slowly decays with two positive components of 350 and 1670 ms (Table 1).

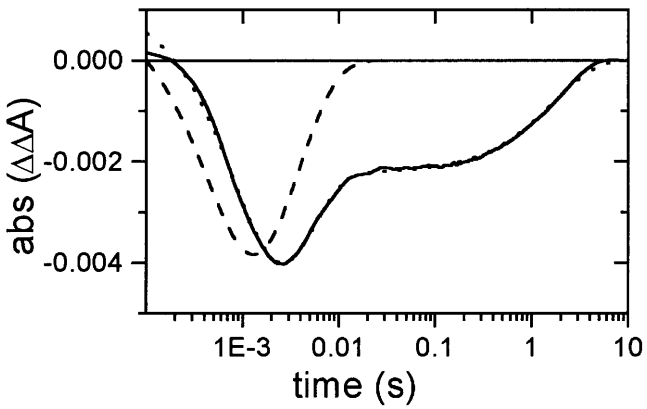

FIGURE 2 Proton release and uptake after bR-state excitation. Solid line: difference of the absorbances with and without pyranine. Lifetime values are given in Table 1. Exciting light: 530 nm flash of Nd-YAG laser. Monitoring light: 450 nm. Solution: 20 μM pm suspension in 0.15 M KCl, pH 7.5, 22°C, 80 μM pyranine. For comparison the pyranine signal is given for wild-type bacteriorhodopsin (*dashed line*).

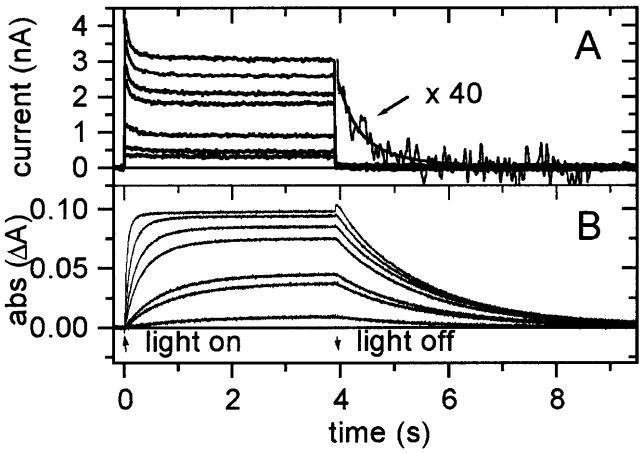

FIGURE 3 Light intensity dependence of electric current and absorbance signals for quasicontinuous illumination with the full spectrum of the 200 W tungsten lamp through neutral filters. (*A*) Electric current. Light intensities from top: 100, 82, 62, 50, 20, 9.7, and 5. The amplified curve shows the average of all decays. (*B*) Absorbencies measured at 632 nm, from top: 100, 20, 9.7, 5, 1, 0.5 and 0.2. Light intensity 100 = 1.97×10^{17} photons cm^{-2} s^{-1}.

In contrast to the time-unresolved current rise, the O-absorbance rise is time-resolved. It becomes faster with increasing light intensity but its amplitude saturates at relatively low light intensities, whereas its decay time remains constant (Fig. 3 *B*). Plateau values for current and absorbance are plotted in Fig. 4 as a function of light intensity. In these measurements, we used the full spectrum of the tungsten lamp. Orange light (>560 nm) as used by Delaney et al. (1995) gave essentially the same results. The light intensity dependence for the plateau of O-absorbance is shown in Fig. 5 *A*, and the rate constants for its rise and decay are shown in Fig. 6 *A*.

Delaney et al. (1995) found that the decay rate of absorbance at 483 nm after flash excitation (10 μs at 550 nm) increases linearly with the light intensity of orange background light (>560 nm). Fig. 6 *B* shows the rate constants for O-decay (measured at 632 nm) after laser flash excitation (at 580 nm) with varying intensity orange background illumination (>560 nm). We note that the light intensity dependence of the rate constants of O-absorbance rise (Fig. 6 *A*) is similar to the rate constants of O-decay (Fig. 6 *B*). The rate constants change linearly with light intensity until ~20 ru, practically until the absorbencies reach saturation. When we compare the maximal O-absorbance for flash excitation (Fig. 5 *B*) with the plateau absorbencies under continuous illumination (Fig. 5 *A*), we also find a similar light intensity dependence but of opposite sign. With light from a xenon lamp with 536 nm band pass filter or with the 514 nm line from an argon ion laser, the results were similar to those with white or orange illumination: O-absorbances saturated early, while the currents continued to increase. However, the ab-

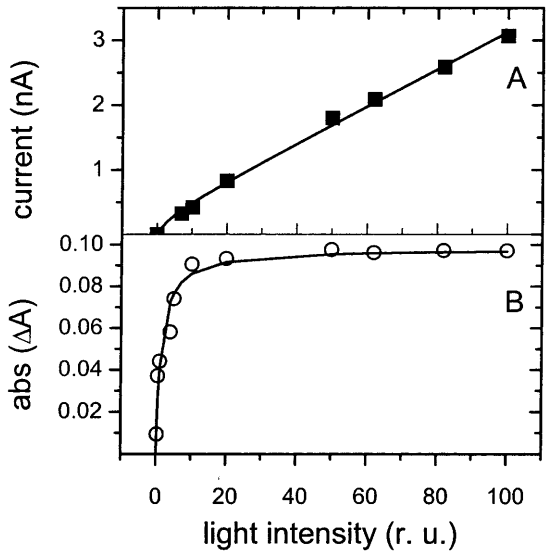

FIGURE 4 Amplitudes of the plateau currents (*A*) and absorbencies (*B*) in Fig. 3, *A* and *B*. Lines show fits with Eqs. 11 and 4 from Appendix, respectively. Light intensity 100 = 1.97×10^{17} photons cm^{-2} s^{-1}.

sorbance rise for the 536 nm light was slower than for orange background light (Fig. 6 *A*, *dashed line*) and the current higher for 514 nm laser light than for the 536 nm band (Fig. 7, *A* and *B*).

These results are unexpected and call into question the conclusion that the cycle ''shortcut'' is due to O-excitation, the explanation preferred by Delaney et al. (1995). Our data

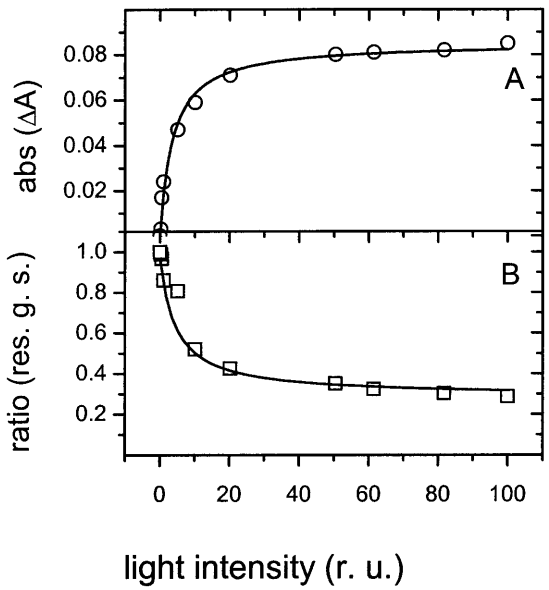

FIGURE 5 (*A*) Plateau absorbencies in orange light (>560 nm) as a function of light intensity. (*B*) Amplitude ratio of the maximal O-absorbance values for flash excitation with and without orange background light, which as Eq. 6 shows, measures the residual ground state bR. Lines are fits with Eqs. 4 and 6 from Appendix, respectively. Light intensity 100 = 1.52×10^{17} photons cm^{-2} s^{-1}.

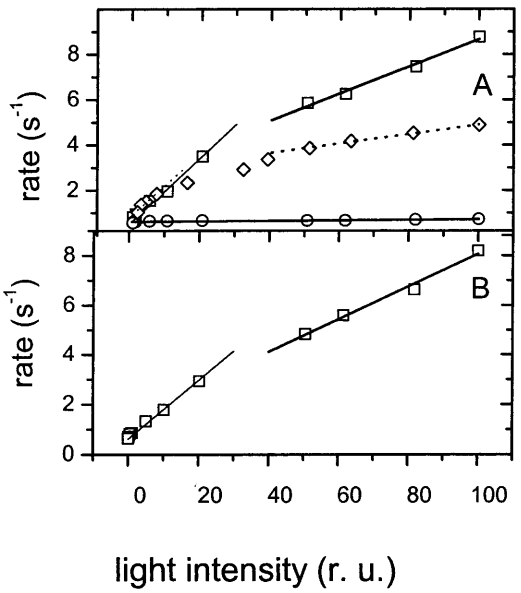

FIGURE 6 (*A*) Rise (*squares*) and decay rate constants (*circles*) of 632 nm absorbance as a function of >560 nm background light intensity; also shown 632 nm absorbance with 514 nm background (*diamonds*). (*B*) Rate constants for O-decay at 632 nm after flash excitation (580 nm) in background light of >560 nm. Lines for light intensities lower than 20 ru are fits with Eq. 3, for higher ones are just to guide the eye. Light intensity 100 = 1.52×10^{17} photons cm^{-2} s^{-1} for >560 nm and 1.8×10^{17} photons cm^{-2} s^{-1} for 514 nm light.

suggest rather that it may originate at the N-component appearing at the start of the cycle slowdown (Delaney et al., 1995). The expected absorbance maximum for N should be close to the ground-state maximum, and Fig. 8 demonstrates that, if we subtract the calculated absorbance changes for the ground state the time course of N- and O-absorbance changes is the same within the limits of our measurements as expected for a fast equilibrium.

Triple flash illumination

The near coincidence of the bR- and N-spectra prevents the use of absorbance measurements to obtain an action spectrum for the ''shortcut.'' However, these intermediates can be distinguished by their electric responses. We used three consecutive 530-nm laser flashes at 100-ms intervals and recorded photocurrents (Fig. 9). (*Note 4:* It is obvious that the selected experimental parameters here are not optimal for our purpose. They were dictated by the available equipment.) At the first flash, all molecules are in the bR state, and the maximal possible current will result. The second flash excites effectively only the residual molecules in the bR state and the N-component of the N↔O equilibrium. Fig. 10 *A* compares the shapes of the first signal (×0.69 to correct for the molecules excited in the first flash) with the second flash signal. Fig. 10 *B* shows the difference and its time integral. Rise and decay can be

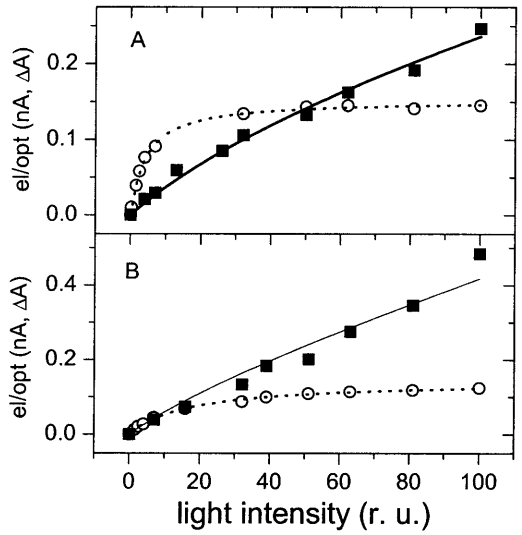

FIGURE 7 Dependence of the current (*squares*) and absorbance (*open circles*) at 632 nm with (*A*) varying green illumination from the xenon lamp with green filter centered at 536 nm. Light intensity 100 = 2.4×10^{17} photons cm^{-2} s^{-1}. (*B*) Varying illumination from the argon ion laser (514 nm). Light intensity 100 = 1.8×10^{17} photons cm^{-2} s^{-1}. Solid lines are fits of the electric current (*squares*) with Eq. 11, dotted lines fits of the absorbencies with Eq. 4 in Appendix.

satisfactorily fit with components of 0.371 ± 0.002 ms and 1.55 ± 0.04 ms, respectively. The difference is positive, indicating charge movement in the pumping direction. This charge transport must be due to excitation of the N-component in the N↔O equilibrium. The transported charge is an order of magnitude smaller than that resulting from the

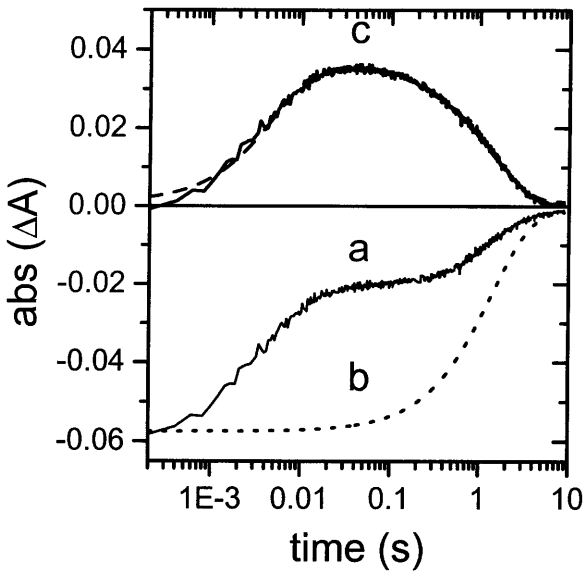

FIGURE 8 Time dependence of absorbance at 550 nm. Curve *a* shows the recorded 550 nm absorbance. Curve *b*, calculated bleaching of bR-state; curve *c*, the difference of *a* and *b* representing absorbance of N intermediate. Nd-YAG laser excitation. Solution: 50 μM $CaCl_2$, pH 7.5, 27°C.

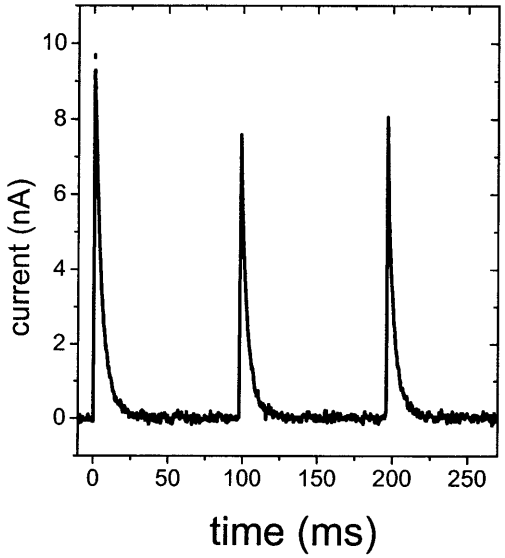

FIGURE 9 Electric responses for three Nd-YAG-laser flashes with 100-ms time delays. Dotted lines are fits with one exponential. The areas of the second and third signal are 0.69 × and 0.73 × that of the first.

excitation of the residual bR, but it shows the kinetics of the "shortcut." The current for the third flash is higher than for the second flash due to the additional bR state generated from N by the second flash and excited by the third flash. Measuring the dependence of the relative increase on the wavelength of the second flash should then yield the action spectrum for the state generating the "shortcut". Fig. 11

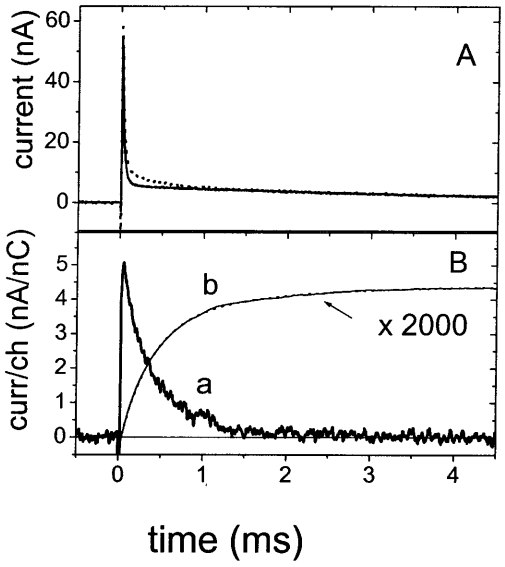

FIGURE 10 (*A*) Current signal for first flash in Fig. 9 × 0.69 (*solid line*) superimposed on current for second flash (*dots*). (*B*) Curve *a*: difference of first flash current × 0.69 and second flash current in Fig. 9, i.e., the electric response due to the excitation of N intermediate. Curve *b*: the time-integral of curve *a*. It was fitted with two exponential components of lifetimes 0.371 (±0.002) and 1.55 (±0.04) ms.

clearly shows that, as expected for N, it is indistinguishable from the bR spectrum at the resolution obtained and its maximum is ~50 nm below the O maximum. Additional data and arguments for this interpretation are presented in the companion paper that describes the photoreactions of O.

DISCUSSION

As pointed out in the Introduction, Delaney et al. (1995) have found that retinal in the O-component of the N↔O equilibrium is still in 13-*cis* configuration, and they convincingly argued that hindered reisomerization to the all-*trans* form causes the accumulation of this intermediate and is relieved by its excitation. Since Delaney et al. had concluded that proton transport is completed in the M→N transition they attributed the high proton-pumping rate of the mutant under continuous illumination to the fast retinal reisomerization through a second photon, probably absorbed by the O-intermediate in N↔O. For this explanation their time-resolved pyranine absorbance measurement is crucial. (This observation represents the only significant difference between their experimental results and ours. Comparing Fig. 1 *C* in Delaney et al. (1995) with Fig. 2 here, it appears possible that a baseline instability indicated in their legend caused the difference.) We have shown here that in the one-photon cycle, net positive charge transport and proton uptake have slow components with kinetics very similar or identical to the slow absorbance decay of O, which is completed only after several seconds with the reestablishment of the bR state. Our action spectrum demonstrates that at 100 ms, significant amounts of N are still present and that the ''shortcut'' originates from the N- and not the O-component of the equilibrium. The absorbance maximum at 590 nm shows that the N↔O equilibrium is shifted far to the right, and at the time of our second flash we are already slightly past the 80 ms maximum of O-absorbance, measured at 632 nm (Fig. 1 *B*). These facts explain the very small amount of charge transport we observe in the photoreaction of N, whereas we should expect that the ~18% of the total charge transport and proton uptake occurring in the thermal decay of O must also occur in the ''shortcut.'' Continuous orange background light, however, will ''drain'' the equilibrium via the N-component and thus restore efficient pumping. (A similar situation has been encountered with M. At room temperature and near neutral pH it occurs only in very low concentrations in the photocycle and is easily overlooked, unless one specifically searches for it. However, the inhibitory effect of blue light on charge transport is easily demonstrated. (Bamberg unpublished).) We interpret the small transient in the O-absorbance with a lifetime of ~300 ms as a transition to a second O-state with either slightly lower and/or blue-shifted absorbance. It is further explored in the accompanying paper on the photoreactions of O.

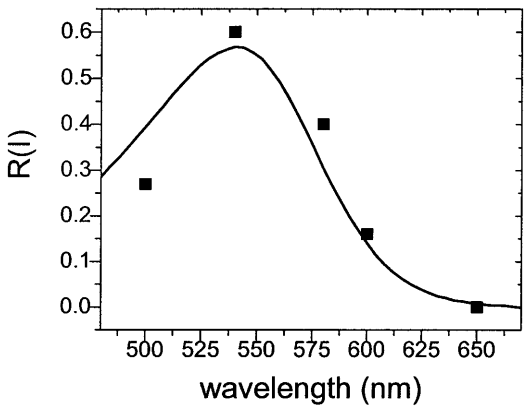

FIGURE 11 Wavelength dependence of the ratio of the charge transported by the third flash, relative to the charge transported by the second flash *R(I)*, i.e., the action spectrum of the ''shortcut.'' The solid line is the absorption spectrum of the ground state of L93A (scaled to *R(I)*).

We note here that photoreactions of N leading back to the ground state via O-like intermediates have been seen in the WTbR photocycle (e. g., Lozier et al., 1978; Váró and Lanyi, 1990; Balashov et al., 1990; Ohtani et al., 1992) and after excitation of WT-N, Váró and Lanyi measured decay times for an O-like intermediate in the same range that we find in L93A. These observations support our assumption that only the kinetics and not the path of the proton through the protein or the sequence of conformational changes have been significantly changed in the mutant.

For additional analysis of our data, we used the equations derived in the Appendix to evaluate the plateau absorbencies and rate constants of the O-absorbance rise in quasicontinuous illumination (Figs. 4–7). Fitting R and σ in Eq. 4 to the points in Figs. 4 *B* and 5 *A* (illumination with the full spectrum of the tungsten lamp and illumination with orange light of >560 nm, respectively) and using the rate-limiting $k_0 = 0.61\ s^{-1}$ of the free O-absorbance decay (Fig. 6 *A*) gave us values for these parameters. The cross sections of photoreaction, σ, are obtained as light intensities and we converted them into average cross sections, $\sigma(a)$, using the wavelength averages 550 nm for white and 590 nm for orange light. The values obtained (Table 2) are comparable to the cross section for photoreaction in WTbR.

We have also estimated the cross sections for cycling from our data for light intensity dependence of maximal O-amplitudes (Fig. 5 *B*) and from O-decay rate constants for laser flash excitation in background light (Fig. 6 *B*). Using Eq. 6 derived from Eq. 1 with different initial conditions, and fitting the parameters as above, we obtained the cross sections in Table 2, row 3. The average cross sections from the two data sets (*rows 2* and *3*) agree well. The cross sections for the full spectrum (*row 1*) are larger because the emission spectrum of the white light covers better the absorption spectrum of L93A with its maximum at 540 nm.

Eq. 3 requires that the rates for the O-absorbance rise under continuous illumination and for the O-decay in background light should increase linearly with light intensity

TABLE 2 Average cross sections (in units of 10^{-16} cm^{-2}) for photocycling bacteriorhodopsin in purple membrane from mutant L93A

Light	$\sigma(a)$ plateau/max	$\sigma(a)$ rise	$\sigma(a)$ decay
White	2.4 ± 0.5	1.7 ± 0.1	
>560 nm	1.2 ± 0.2	0.9 ± 0.1	
Flash 580 nm	0.9 ± 0.1		0.8 ± 0.1

Average cross sections $\sigma(a)$ (for definition see Discussion) are calculated from absorbances measured at 632 nm in light from a tungsten lamp either with the full spectrum (*white*) or through 560 nm high pas filter (>560 nm). The last row shows results from laser flash excitation at 580 nm in >560 nm background light. First column presents $\sigma(a)$ values calculated from plateaus for quasicontinuous illumination or maxima of absorption for flash excitation. Second column contains $\sigma(a)$ values calculated from rise of absorbencies. Third column gives $\sigma(a)$ calculated from the decay of flash excited absorbencies.

and, when extrapolated to zero light intensity, the rate of free O-decay k_0 should be obtained. The data for orange light in Fig. 6 and similar data for white light (not shown) fulfill these requirements for light intensities lower than 20 ru, i.e., 0.5×10^{17} photons cm^{-2} s^{-1}. Values for $\sigma(a)$, obtained from these data, are also shown in Table 2. The agreement of the average cross sections calculated from the two different data sets validates our analysis. Here we note that the light intensity dependence of the rate constant in Fig. 2 of the paper of Delaney et al. (1995) is fully explained by Eq. 6 in the Appendix. The ''shortcut'' at O, which they assumed, is not necessary.

It may appear inconsistent using single photon equations (Eqs. 3, 4, and 6) to describe the saturation and rate constants of O absorption while serious deviations appear in the rate constants from linearity at higher light intensities (Fig. 6). Using these equations we followed the analysis of Delaney et al. (1995). The correct description of all events including the photocurrent should be based on equations including double photon excitation. The observation that O saturates at low light intensities where the rate constants increase linearly determines an apparent ''single photon'' range. The occurrence of deviation from linearity (Fig. 6) and the increase of the photocurrent indicate the region of the ''double photon'' processes.

The fast rise and decay of the electric current in Fig. 3 due to the main current components with lifetimes of 6.3 ms coincide with the N and O rise (see Fig. 1). The current rise at higher light intensities overshoots and then falls back to a photosteady state equilibrium (plateau) value. The contribution of the two slowest components to the plateau current is negligible but detectable after the decay of the main component (Fig. 3).

We see in Figs. 3, 4, and 7 that the plateau current increases more or less linearly throughout the light intensity range, whereas the O-absorbance saturates at low light intensities. These results, especially the continuous increase of the current for 514 nm excitation (Fig. 7), are consistent with the assumed acceleration of the photocycle, confirming it with a different method (Delaney et al., 1995), but the wavelength of the second photon is much closer to the absorbance maximum of N (or bR) than O.

Eq. 11 describes the two-photon processes and will apply equally to N and O if they are in rapid equilibrium. Fitting Eq. 11 to the data for the electric current in Fig. 4 and 7, we obtained the average cross section ratios of photoreactions: $\sigma_G/\sigma_I = 2.5 \pm 1.4$ for white light (Figs. 3 and 4), 1.02 ± 0.38 for the green broad band, and 0.67 ± 0.53 for the 514 nm laser line (Fig. 7). (The lines in these figures are the fits of Eq. 11 to the data). Though the errors are rather large, these data still confirm our conclusion. Obviously the cross sections are nearly equal at 514 nm. The white light and the filtered illumination from the xenon lamp contain substantial red. For these components the average cross section for the O intermediate should be large and the cross section ratio should decrease contrary to the observed data. From these ratios we also infer that the ''shortcut'' apparently originates at the N-component of the equilibrium.

The current overshoots at the onset of illumination (Fig. 3) and the break in the rate versus light intensity curve, which occurs when O-concentration reaches its maximum (Fig. 6), result from the complicated cycle kinetics. When the light is turned on, all molecules are in the bR-state, which must produce the maximal possible current for that light intensity within the bR to N↔O transition time; which produces 80% of the total current for one cycle turnover. However, the N↔O equilibrium for this light intensity is fast established and the current falls slightly and stabilizes at the plateau value. At higher intensities more bR is excited and more of N is rapidly returned to bR and again excited increasing the plateau current and the cycling rate. However, some will drain via the N↔O equilibrium into O-state and return to bR thermally and also by excitation (see the next paper in this issue) producing little additional current, but still increasing the amount available for a second excitation of the bR-state and the rate of current production. When the light is turned off, fast photoconversion of N stops and all molecules, still in the cycle, return via O to bR, causing the transient increase in O-absorbance. The increase is only seen at the higher light intensities, but the kinetics for the free O-decay does not change (Fig. 3 *B*).

Our experimental results differ from those published by Subramaniam and collaborators (Subramaniam et al., 1991, 1997, 1999; Delaney et al., 1995; Delaney and Subramaniam, 1996) in the following points: 1), Proton reuptake is completed only in the O to bR transition. 2), A second O-like intermediate has been detected in the decay of the O-component, which is further explored in the following paper (Tóth-Boconádi et al., 2003). And 3), The effect of continuous illumination and background light on the O-lifetime is the fast reset not of O but of N by absorption of a second photon. However, these differences do not invalidate the important conclusion of these authors, namely, that in WTbR,

the contact between the 13-methyl of retinal and a terminal methyl of Leu-93 is important for fast *cis-trans* retinal isomerization and that its lack causes the slowdown in the photocycle of L93A.

APPENDIX

In a continuous light of light intensity Φ photons $cm^{-2}\ s^{-1}$, the change of the number n (normalized to one) of photocycling molecules is described by the following differential equation:

$$dn/dt = \sigma\Phi(1 - n) - k_0 n, \quad (1)$$

where σ is the cross section of the photoreaction and k_0 the rate constant of the rate-limiting step, in this case that of the decay of N + O mixture. The solution is

$$n(t) = (\sigma\Phi/(\sigma\Phi + k_0))(1 - e^{-(\sigma\Phi + k_0)t}). \quad (2)$$

The fraction of the cycling molecules grows as 1 − exponential with rate constant

$$k = \sigma\Phi + k_0 \quad (3)$$

and reaches an equilibrium

$$E = R(\sigma\Phi/(\sigma\Phi + k_0)), \quad (4)$$

where R is a scaling factor.

Figs. 5 and 6, panels B, contain data on the light intensity dependence of the maximal amplitudes and of the rate constants of the decay of O for laser flash excitation. The process in background light is described by Eq. 1, too, but with different initial condition. In background light of light intensity Φ photons $cm^{-2}\ s^{-1}$, $R(\sigma\Phi/(\sigma\Phi + k_0))$ molecules are already cycling, leaving $R(1 - \sigma\Phi/(\sigma\Phi + k_0))$ excitable molecules. We took the time of laser excitation as $t = 0$ when the laser excites a fraction a of the excitable molecules. The number of photocycling molecules is:

$$N(0) = R(\sigma\Phi/(\sigma\Phi + k_0) + a(1 - \sigma\Phi/(\sigma\Phi + k_0))). \quad (5)$$

Then with this initial condition, the number of molecules driven by laser in background light decays as:

$$N(t) = Ra(1 - \sigma\Phi/(\sigma\Phi + k_0))\, e^{-(\sigma\Phi + k_0)t}. \quad (6)$$

It is seen that Eq. 6 contains similar expressions for the variation of the rate constant and the maximal amplitude (at $t = 0$) as Eq. 3 and 4.

We now extend the equation for two-photon reaction. Let B_0 be the concentration of all molecules, B of those in the ground state, N and O of the intermediates, and σ_G and σ_I the cross sections for excitation of B and N or O, respectively. We write the equation so that σ_I is for N in equilibrium with O with rates k_1 and k_{-1}. The decay of O goes with rate k_0. Then having

$$B_0 = B + N + O, \quad (7)$$

the time dependencies of the species are

$$dB/dt = -\sigma_G\Phi B + k_0 O + \sigma_I\Phi N \quad (8)$$

$$dN/dt = \sigma_G\Phi B - \sigma_I\Phi N - k_1 N + k_{-1} O \quad (9)$$

$$dO/dt = k_1 N - k_{-1} O - k_0 O. \quad (10)$$

It is easy to calculate the concentration of the species in equilibrium at a given light intensity Φ. The current in this special case originates mainly from the short-living M. Fig. 3 shows that the remaining long-living current component due to N + O mixture after switching off the light is ~1% of that in light. Fig. 10 shows that the N current due to ''shortcut'' is ~20 times smaller than the current due to the photocycle. Thus, we may take that the current is mainly due to the M component and proportional to $\sigma_G\Phi B$, i.e.,

$$I = C \times ((\sigma_G\sigma_I\Phi^2 + \sigma_G\Phi k_0)/((2\sigma_G + \sigma_I)\Phi + k_0)). \quad (11)$$

Here C is a normalizing factor. We assumed that the rates k_1 and k_{-1} are equal and much larger than k_0.

We now discuss how the action spectrum was calculated from the triple flash experiment. Two measurements were made: 1), Double flash: first flash at $t = 0$ (area proportional to the charge $F_1(2)$) and second flash at $t = 200$ ms ($(F_3(2)$). And 2), Triple flash: first flash at $t = 0$ ($F_1(3)$), second flash at $t = 100$ ms ($F_2(3)$), and third flash at $t = 200$ ms ($F_3(3)$). Let B be the number of bR molecules, σ_G the cross section for ground state excitation at 530 nm, $\sigma_{G\lambda}$ at the measuring wavelength λ, σ_I the cross section for the intermediate state excitation at 530 nm, and $\sigma_{I\lambda}$ at the measuring wavelength λ, then

$$F_1(2) \quad \text{or} \quad F_1(3) = A_1 B\sigma_G\Psi_1; \quad (12)$$

$$F_3(2) = A_1 B(1 - \sigma_G\Psi_1)\sigma_G\Psi_1 + A_2 B\sigma_G\Psi_1\sigma_I\Psi_1; \quad (13)$$

and

$$F_2(3) = A_1 B(1 - \sigma_G\Psi_1)\sigma_{G\lambda}\Psi_2 + A_2 B\sigma_G\Psi_1\sigma_{I\lambda}\Psi_2. \quad (14)$$

Ψ_1 and Ψ_2 are the photon numbers cm^{-2} of the Nd-YAG laser and the second laser, A_1 and A_2, are to point out that the electric answers differ for the ground and intermediate states. We assume the charge due to the intermediate negligible (according to Fig. 10, <10%, thus $A_2 \approx 0$). With this assumption

$$\begin{aligned} F_3(3) &= A_1 B(1 - \sigma_G\Psi_1)\sigma_G\Psi_1 \\ &\quad - A_1 B(1 - \sigma_G\Psi_1)\sigma_{G\lambda}\Psi_2 + A_1 B\sigma_G\Psi_1\sigma_{I\lambda}\Psi_2 = \\ &= F_3(2) - F_2(3) + F_1(3)\sigma_{I\lambda}\Psi_2. \end{aligned} \quad (15)$$

From Eqs. 12–15, a quantity proportional to $\sigma_{I\lambda}$, containing only measured quantities (areas of the electric signals and Ψ_2), can be calculated:

$$R(I) = (F_3(3)/F_1(3) - F_3(2)/F_1(3) + F_2(3)/F_1(3))/\Psi_2. \quad (16)$$

(For the sake of simplicity, we omitted, in addition to quantities multiplied by A_2, also the regeneration of the excited bR-state molecules in the description being in the % range. The correct calculation does not change more than 5%, the measured data applied in Eq. 14 take them into account. These simplifications do not allow consideration of the $R(I)$ values as accurate cross sections for N excitation, however.)

We thank Prof. S. Subramaniam, who provided the L93A mutant, Profs. E. Bamberg and R. A. Bogomolni for permission to quote their unpublished observations and for discussions, Dr. A. Dér for help in calculations, and Mr. L. Oroszi for computer program. Prof. Bogomolni also maintained the L93A strain in his laboratory.

This work was supported by the Hungarian National Science Fund OTKA T025236 and by North Atlantic Treaty Organization grant CRG 930419.

REFERENCES

Balashov, S. P., E. S. Imasheva, F. F. Litvin, and R. H. Lozier. 1990. The N intermediate of bacteriorhodopsin at low temperature: stabilization and photoconversion. *FEBS Lett.* 412:93–96.

Chizhov, I., M. Engelhard, D. S. Chernavskii, B. V. Zubov, and B. Hess. 1992. Temperature and pH sensitivity of the O640 intermediate of the bacteriorhodopsin photocycle. *Biophys. J.* 61:1001–1006.

Chizhov, I., D. S. Chernavskii, M. Engelhard, K. H. Mueller, B. V. Zubov, and B. Hess. 1996. Spectrally silent transitions in the bacteriorhodopsin photocycle. *Biophys. J.* 71:2329–2345.

Delaney, J. K., U. Schweiger, and S. Subramaniam. 1995. Molecular mechanism of protein-retinal coupling in bacteriorhodopsin. *Proc. Natl. Acad. Sci. USA*. 92:11120–11124.

Delaney, J. K., and S. Subramaniam. 1996. The residues Leu 93 and Asp 96 act independently in the bacteriorhodopsin photocycle: studies with Leu93-Ala, Asp96-Asn double mutant. *Biophys. J.* 70:2366–2372.

Dér, A., P. Hargittai, and J. Simon. 1985. Time resolved photoelectric and absorption signals from oriented purple membranes immobilized in gels. *J Biochem. Biophys. Methods.* 10:295–300.

Dioumaev, A. K., L. S. Brown, R. Needleman, and J. K. Lanyi. 2001. Coupling of the reisomerization of the retinal, proton uptake, and reprotonation of Asp-96 in the N photointermediate of bacteriorhodopsin. *Biochemistry*. 40:11308–11317.

Ebrey, T. G. 1993. Light energy transduction in bacteriorhodopsin. *In* Thermodynamics of Membrane Receptors and Channels. M. B. Jackson, editor. CRC Press, Boca Raton, FL. 354–387.

Keszthelyi, L., and P. Ormos. 1989. Protein electric response signals from dielectrically polarized systems. *J. Membr. Biol.* 109:193–200.

Lanyi, J. K. 1993. Proton translocation mechanism and energetics in the light-driven pump bacteriorhodopsin. *Biochim. Biophys. Acta*. 1183: 241–261.

Lanyi, J. K. 1997. Mechanism of ion transport across membranes. Bacteriorhodopsin as a prototype for proton pump. *J. Biol. Chem.* 272:31209–31212.

Lozier, R. H., H. W. Niederberger, M. Ottolenghi, G. Sivorinovsky, and W. Stoeckenius. 1978. On the photocycles of light- and dark-adapted bacteriorhodopsin. *In* Energetics and Structure of Halophilic Microorganisms. S. R. Caplan and M. Ginzburg, editors. Elsevier/North-Holland Biomedical Press, New York. 123–141.

Luecke, H. 2000. Atomic resolution structures of bacteriorhodopsin photocycle intermediates: the role of discrete water molecules in the function of this light-driven ion pump. *Biochim. Biophys. Acta*. 1640:133–156.

Ohtani, H., H. Itoh, and T. Shinmura. 1992. Time-resolved fluorometry of purple membrane of Halobacterium halobium. *FEBS Lett.* 306:6–8.

Stoeckenius, W. 1999. Bacterial rhodopsins: evolution of a mechanistic model for the ion pump. *Protein Sci.* 8:447–459.

Subramaniam, S., A. R. Faruqi, D. Oesterhelt, and R. Henderson. 1997. Electron diffraction studies of light-induced conformational changes in the Leu 93-Ala bacteriorhodopsin mutant. *Proc. Natl. Acad. Sci. USA*. 94:1767–1772.

Subramaniam, S., D. A. Greenhalgh, P. Rath, K. J. Rotschild, and H. G. Khorana. 1991. Replacement of leucine-93 by alanine or threonine slows down the decay of the N and O intermediates in the photocycle of bacteriorhodopsin: implications for proton uptake and 13-cis-retinal →all-trans-retinal reisomerization. *Proc. Natl. Acad. Sci. USA*. 88:6873–6877.

Subramaniam, S., M. Lindahl, P. Bullough, A. R. Faruqi, J. Tittor, D. Oesterhelt, L. Brown, J. Lanyi, and R. Henderson. 1999. Protein conformational changes in the bacteriorhodopsin photocycle. *J. Mol. Biol.* 287:145–161.

Tóth-Boconádi, R., L. Keszthelyi, and W. Stoeckenius. 2003. Photoexcitation of the O-intermediate in bacteriorhodopsin mutant L93A. *Biophys. J.* 84:3857–3863.

Váró, G., and J. K. Lanyi. 1990. Pathways of the rise and decay of the M photointermediate(s) of bacteriorhodopsin. *Biochemistry*. 29:2241–2250.